

Cardiac CINE Imaging with “Dixon” Water-Fat Separation and Steady-State Free Precession

S. B. Reeder¹, M. Markl¹, H. Yu¹, J. C. Hellinger¹, R. J. Herfkens¹, N. J. Pelc¹

¹Stanford University, Stanford, CA, United States

Introduction: Steady-state free precession (SSFP) is a rapid, short TR imaging technique with high SNR and excellent blood-myocardial contrast (1). For these reasons, SSFP has gained recent widespread use for cardiac CINE imaging. Conventional SSFP is limited by the fact that water and fat both appear bright and are difficult to distinguish, possibly obscuring underlying pathology such as pericardial disease, fatty infiltration seen with arrhythmogenic right ventricular dysplasia (ARVD), or lipomatous myocardial neoplasms. Currently, there are no fat suppression techniques that have been applied to cardiac CINE SSFP imaging, and fat suppression techniques used with other SSFP applications are impractical for implementation with cardiac SSFP imaging and are sensitive to field inhomogeneities (2-4).

“Dixon” water-fat decomposition methods achieve uniform separation of fat from water even in the presence of field inhomogeneities (5). Increasing the TE of SSFP, however, also increases the minimum TR, and consequently, implementation of “Dixon” techniques with SSFP has been limited because SSFP requires short TRs to prevent image degradation from banding and flow artifacts caused by field inhomogeneities. These factors limit TE increments to small values not used with typical “Dixon” water-fat decomposition methods (5). To address this challenge, water and fat CINE cardiac images were decomposed from multi-coil SSFP images using an iterative least-squares algorithm, formulated for fitting data from images acquired at short TE values (6).

Theory: SNR dependence on evenly spaced echo times with TE increment, Δt , for a water-fat decomposition has been described using the effective number of signal averages (NSA) which is maximized when $\Delta t=1.5\text{ms}$ at $1.5T$ for a 3-point acquisition, and the fat-water chemical shift is -220Hz (5,6). Unfortunately, this increment increases the minimum TR by 3.0ms, and causes substantial banding and flow related artifacts. It becomes necessary, therefore, to decrease the TE increment, trading off some SNR performance for a decrease in TR and reduction of artifacts. We have recently described an iterative least-squares water-fat decomposition approach that uses a generalized algorithm for decomposing water and fat from multi-coil images acquired at short echo times (6). This facilitates the acquisition of SSFP images with short TRs and minimal banding artifacts.

Methods: Image acquisition was performed at 1.5T (Signa CV/i, GEMS, Milwaukee, WI) with a retrospectively ECG-gated CINE SSFP sequence that acquires sequential sets of CINE images at 3 different echo times. A phased array torso coil was used in 3 volunteers (2 M, 1 F; age (yrs): 31-33, mean 31.7) and 13 patients (9 M, 4 F; age (yrs): 39-66, mean 54.6) except for one large patient (body coil). Informed consent was obtained from all individuals and the study was approved by our IRB. Imaging parameters included: $\alpha=50^\circ$, $BW=\pm 125\text{kHz}$; $FOV=32\text{-}38\text{cm}$; $\text{slice}=8\text{mm}$; $N_x=224\text{-}256$ (partial echo); $N_y=128$; views per segment (N_{seg})=12-16, temporal resolution=60-80ms. 20 CINE phases were retrospectively reconstructed and breath-hold time was 20-27 heartbeats per slice. Automated shimming routines were used for all imaging. In one volunteer, 3-point acquisitions were obtained with the TE increment varied from 0.3-1.4ms (TR=3.8-6.0ms), to measure the NSA behavior of the water-fat decomposition. In all other studies, the TE increment was 0.9ms and the three values of TE were approximately TE=0.8, 1.7, 2.6ms, with TR=4.7-5.2ms.

Results: Fig. 1 plots the measured NSA for myocardium and subcutaneous fat, against TE increment. Measurements were averaged over all 20 cardiac phases, and are plotted with the theoretical NSA behavior (5,6), demonstrating excellent agreement. Images with TE increment greater than 1.4ms were markedly degraded by artifact due to the associated TR increase. Fig. 2 shows an example of water-fat separation in a patient with a pathology proven interventricular septal lipoma, and Fig. 3 shows a patient with chronic pericarditis on steroid therapy. Uniform water-fat separation was achieved in all images from all studies. Subjective evaluation of images in all 16 studies found that images acquired with TR of approximately 5ms or less had good image quality with acceptable levels of banding and flow artifacts.

Discussion: Selection of TE increment was a tradeoff between SNR performance and adequate image quality of the source images. It can be shown that a TE increment of 0.9ms decreases SNR by 17% from the maximum, and additional decreases lead to more substantial decreases in SNR (5,6). At 1.5T, an increment of 0.9ms was a good compromise because it facilitated a TR of 5ms or less, to maintain low levels of artifact, with a low cost to SNR performance of the water-fat decomposition.

Breath-holding is necessary to ensure that source images acquired at different echo times are spatially registered, and the major limitation of this method is that it lengthens the breath-hold duration three-fold, limiting the achievable spatial and temporal resolution of this method. Future work will focus on methods such as parallel imaging that reduce the required data to decompose fat from water, reducing minimum breath-hold times and improving spatial and/or temporal resolution.

Conclusion: Multi-coil “Dixon” techniques using an iterative least-squares fitting algorithm can be combined with SSFP cardiac CINE imaging to obtain water and fat images with excellent water-fat separation. This improves visualization of water and fat structures within and around the heart while retaining the high CNR of SSFP imaging. This approach holds potential for clinical imaging applications that require uniform water-fat separation such as ARVD, lipomatous cardiac neoplasms, pericardial disease, and possibly coronary artery angiography..

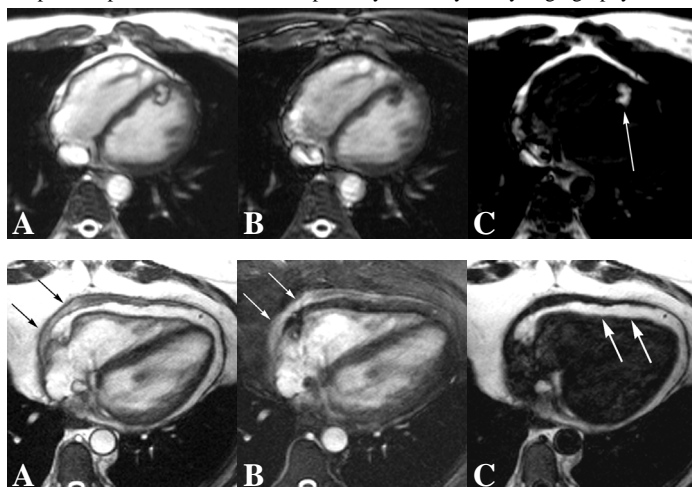
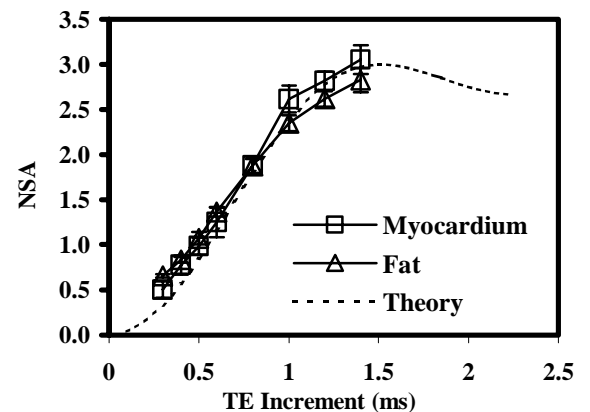


Fig 1: (above) Measured NSA plotted against TE increment for myocardium and fat. Theoretical values are plotted as a dashed line.

Fig 2: (left) Axial source (a), water (b), and fat (c) images for one of 20 time frames from a patient with a pathology proven lipoma of the ventricular septum (arrow).

Figure 3 (lower left): Axial source (a), water (b), and fat (c) images for one of 20 time frames from a patient with chronic pericarditis. Thick pericardium (small black/white arrows) separates pericardial fat (large white arrows) from epicardial fat.

References:

1. Oppelt, A. *Electromedica* 1986;3:15-18
2. Scheffler et al, 2001;45(6):1075-1080
3. Vasanawala et al, *MRM*,1999;42(5):876-883
4. Vasanawala et al, *MRM*, 2000;43(1):82-90
5. Glover et al, *JMRI*, 1:521-530.
6. Reeder et al, *MRM* 2003, *in press*.

Acknowledgments: The authors wish to thank Garry Gold, MD; Angel Pineda, PhD; Mary Draney, PhD; and Jean Brittain, PhD for their assistance, and to acknowledge support from NIH grant P41 RR09784, the Lucas Foundation, GE Medical Systems and The Phil N. Allen Trust.